# MIKE 3 Flow Model FM

## Hydrodynamic module

## Non-hydrostatic formulation

### Validation Report

# PLEASE NOTE

**COPYRIGHT**

This document refers to proprietary computer software, which is protected by copyright. All rights are reserved. Copying or other reproduction of this manual or the related programmes is prohibited without prior written consent of DHI A/S (hereinafter referred to as "DHI"). For details please refer to your 'DHI Software License Agreement'.

**LIMITED LIABILITY**

The liability of DHI is limited as specified in your DHI Software License Agreement:

In no event shall DHI or its representatives (agents and suppliers) be liable for any damages whatsoever including, without limitation, special, indirect, incidental or consequential damages or damages for loss of business profits or savings, business interruption, loss of business information or other pecuniary loss arising in connection with the Agreement, e.g. out of Licensee's use of or the inability to use the Software, even if DHI has been advised of the possibility of such damages.

This limitation shall apply to claims of personal injury to the extent permitted by law. Some jurisdictions do not allow the exclusion or limitation of liability for consequential, special, indirect, incidental damages and, accordingly, some portions of these limitations may not apply.

Notwithstanding the above, DHI's total liability (whether in contract, tort, including negligence, or otherwise) under or in connection with the Agreement shall in aggregate during the term not exceed the lesser of EUR 10.000 or the fees paid by Licensee under the Agreement during the 12 months' period previous to the event giving rise to a claim.

Licensee acknowledge that the liability limitations and exclusions set out in the Agreement reflect the allocation of risk negotiated and agreed by the parties and that DHI would not enter into the Agreement without these limitations and exclusions on its liability. These limitations and exclusions will apply notwithstanding any failure of essential purpose of any limited remedy.

# CONTENTS

MIKE 3 Flow Model FM
Hydrodynamic Module, Non-hydrostatic formulation
Validation Report

# 1 Vision and scope

The hydrodynamic module in MIKE 3 Flow Model FM is based on the numerical solution of the three-dimensional incompressible Reynolds averaged Navier-Stokes equations invoking the assumptions of Boussinesq. Both the full 3D Navier-Stokes equations and the 3D shallow water equations can be applied. The latter invokes the hydrostatic pressure assumption. Thus, the model consists of continuity, momentum, temperature, salinity and density equations and is closed by a turbulent closure scheme. In the horizontal domain both Cartesian and spherical coordinates can be used. The free surface is taken into account using a sigma-coordinate transformation approach.

A set of well-defined test cases for MIKE 3 Flow Model FM have been established. The test-suite is used for validation. The main focus is validation of the non-hydrostatic formulation. For comparison a number of simulations are also performed using the hydrostatic formulation.

# 2 Validation Test Cases

## 2.1 Internal Seiche

### 2.1.1 Description

This test case deals with oscillations of the internal seiche in a closed basin. This test case is similar to the internal seiche case studied by Vitousek and Fringer (2014). The initial density stratification as function of the x- and z-coordinate is given by

$$S(x,z) = \frac{(S_1 + S_2)}{2} + \frac{(S_1 - S_2)}{2} tanh\left[\frac{2tanh^{-1}\alpha_s}{\delta}\left(z + \frac{D}{2} - acos(kx)\right)\right]$$

where $S_1$ and $S_2$ are the salinity at the top and bottom, respectively, $D$ is the depth of the basin, $a$ is the amplitude of the seiche, $k$ is the horizontal wave number, $\delta$ is the internal thickness, and $\alpha_s$=0.99. For large water depth the wave number $k = \pi/L$, where L is the length of the basin. The temperature is constant and the density is obtained using the UNESCO equation of state (see UNESCO,1981).

Simulation is performed in a closed basin with $L = 10m$ and $D = 16m$. The width of the basin is 1m. For the initial density stratification $S_1 = 6.71866kg/m^3$, $S_2 = 19.7178kg/m^3$, $\delta = 1m$ and $a = 0.1m$ is applied. A reference density $\rho_0 = 1010 \, PSU$ is aplied. With $T = 10°$ the density at the top and bottom is $1004.5 \, PSU$ and $1015.5 \, PSU$, respectively, and the density difference is then $\Delta\rho/\rho_0 = 0.01$. The initial density stratification is illustrated in Figure 2.1.
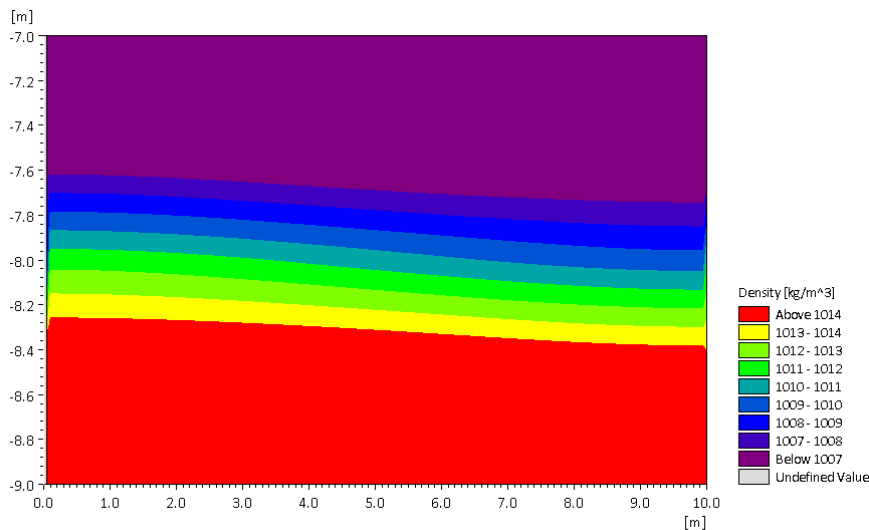


Figure 2.1    Vertical cross section of the initial density

### 2.1.2 Setup

The horizontal mesh consists of uniform quadrilateral elements with one element across the basin and 200 elements along the basin. In the vertical 40 equidistant sigma layers are applied. The duration time for the simulation is 120s and the average time step is 0.001s for the flow calculation and 0.002s for the temperature and salinity calculation.

No Coriolis force is applied, and no horizontal and vertical eddy viscosity are applied.

Simulations are performed using both the non-hydrostatic and hydrostatic version of MIKE 3 Flow Model FM. For the hydrostatic version the higher-order scheme in time and space is applied.

### 2.1.3    Results

The response of the free surface at x=0 to the internal seiche is shown in Figure 2.2. The response consists of two oscillation modes. The first mode corresponds to the frequency of the internal seiche and the second mode corresponds to the natural frequency of the free-surface seiche. It can be seen that the hydrostatic simulation underpredicts the amplitudes and overpredicts the frequencies compared to the non-hydrostatic simulation.
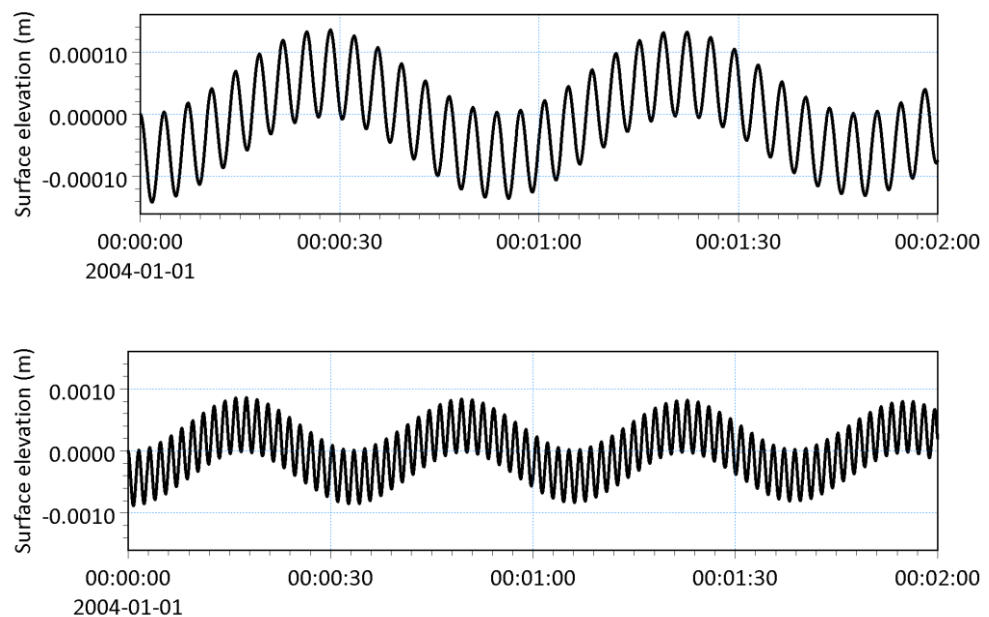


Figure 2.2    Response of the fee-surface at x=0 to the internal seiche. Top figure: Non-hydrostatic simulations. Bottom figure: Hydrostatic simulation.

## 2.2    Lock-exchange

### 2.2.1    Description

A regular tank is filled by two fluids of different density and the fluids are initially separated by a vertical gate at the centre of the tank. When the water is released from rest, then the denser saline water will be driven under the lighter water body during a so-called lock exchange process. The velocity across the interface is of opposite sign. At the interface a chain of well-defined vortices will be developed due to the Kelvin-Helmholtz instability.

For this test the configuration used by Härtel et al. (2000), Fringer et al. (2006) and Lai et al. (2010) is applied. The length of the tank is 0.8m and the width is 0.01m. The initial water depth is constant 0.1m. Initially, the channel is filled with stagnant water ($u=v=w=0$), but with varying salinity $S_1$=5PSU and $S_2$=6.31003PSU. The temperature is 10°C. Hence, the resulting densities of the two fluids are $\rho_1$=1003.61kg/m$^3$ and $\rho_2$=1004.63kg/m$^3$, respectively and the density difference $\Delta\rho$=1.02kg/m$^3$.

## 2.2.2 Setup

The horizontal mesh consists of uniform quadrilateral elements with one element across the tank and 400 elements along the tank. In the vertical 100 equidistant sigma layers are applied. The duration time for the simulation is 180s and the average time step is 0.0008s for the flow calculation and 0.01s for the temperature and salinity calculation.

No Coriolis force is applied, and no horizontal and vertical eddy viscosity are applied. The Riemann factor is set to 0.2 for the HLLC solver.

Simulations are performed using both the non-hydrostatic and hydrostatic version of MIKE 3 Flow Model FM. For the hydrostatic version the higher-order scheme in time and space is applied.

## 2.2.3 Results

Figure 2.3 shows the density field at T=12s, 18s and 27s using the non-hydrostatic version of MIKE 3 Flow Model FM. The results presented here compare very well with the results presented by Lai et al. (2006) both with respect to the propagation speed of the front and the formation of the vortices. Figure 2.4 shows the density field at T=12s, 18s and 27s using the hydrostatic version of MIKE 3 Flow Model FM. The hydrostatic version is able to model the primary lock exchange flow, but it is not possible to model the formation of vortices and the front speed is also overpredicted by approximately 8%.
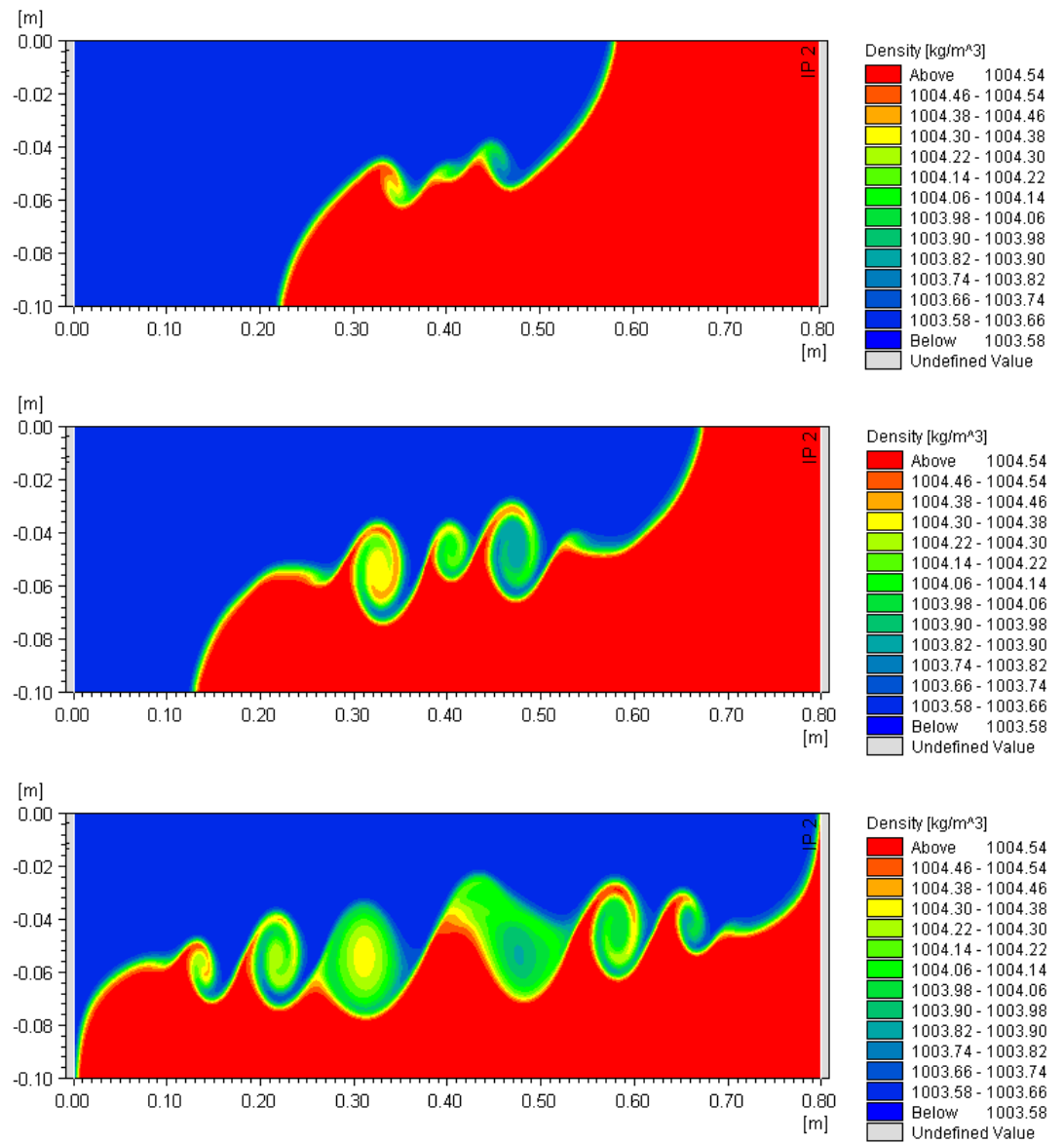
Figure 2.3    Vertical cross section showing the density field at T=12, 18 and 27 (top to bottom). Simulation performed using the non-hydrostatic version of MIKE 3 Flow Model FM.
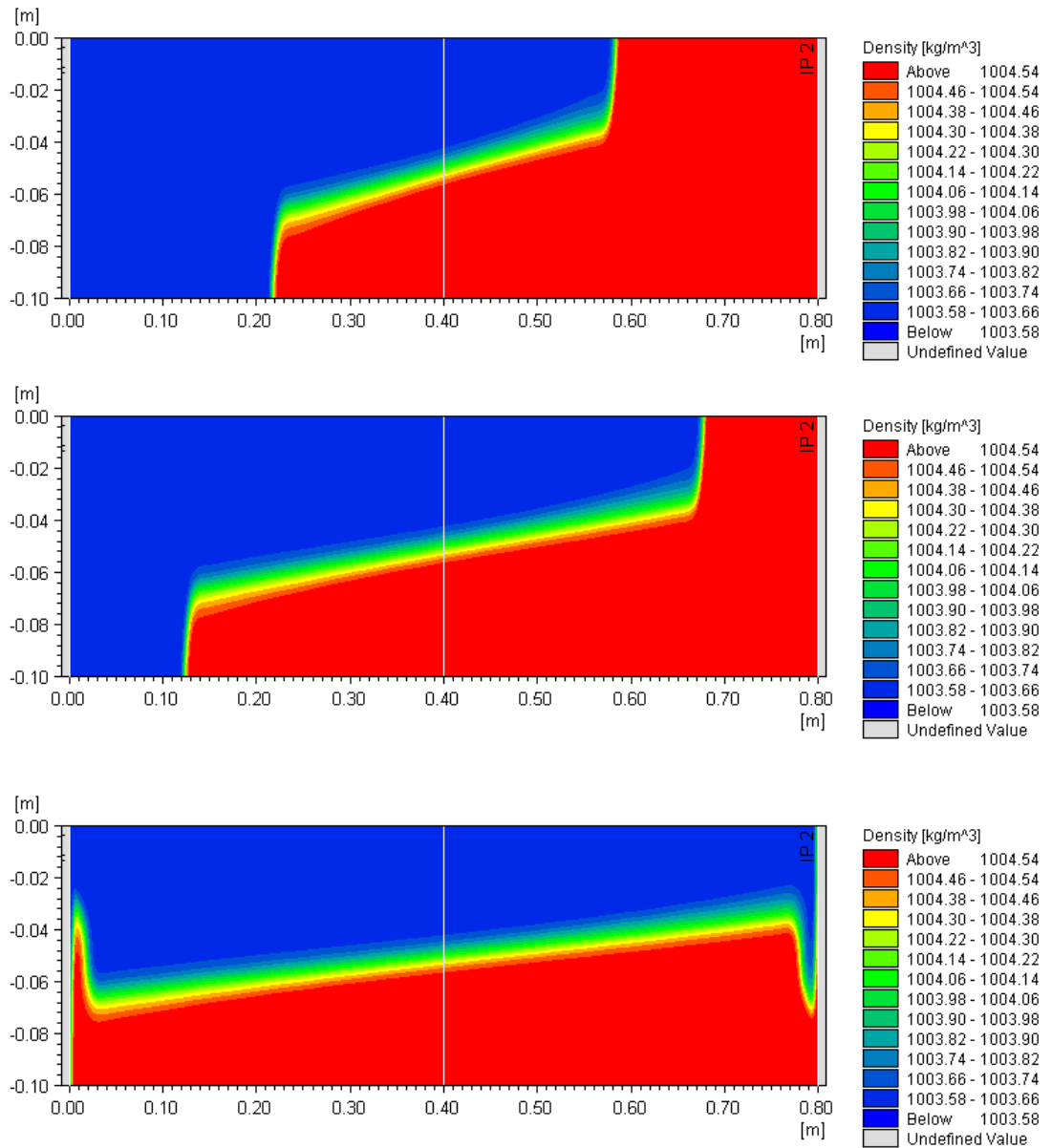
Figure 2.4    Vertical cross section showing the density field at T=12, 18 and 27 (top to bottom).
Simulation performed using the hydrostatic version of MIKE 3 Flow Model FM.

## 2.3    Internal Solitary Wave

### 2.3.1    Description

This test case is a simulation of the laboratory experiments described in Horn et al.
(2001). A regular tank is tilted about a horizontal axis through the centre of the tank. The
tank is filled by two fluids at rest with different density such that the heavier fluid lies below
the lighter fluid. The experiment is started by tilting the tank back to horizontal resulting in
a density gradient driving the fluid flow. This results in an initial condition with two fluids of

different density with a planar interface that is rotated $\theta$ degrees about a horizontal axis and an interface depth $h$ (see Figure 2.5).
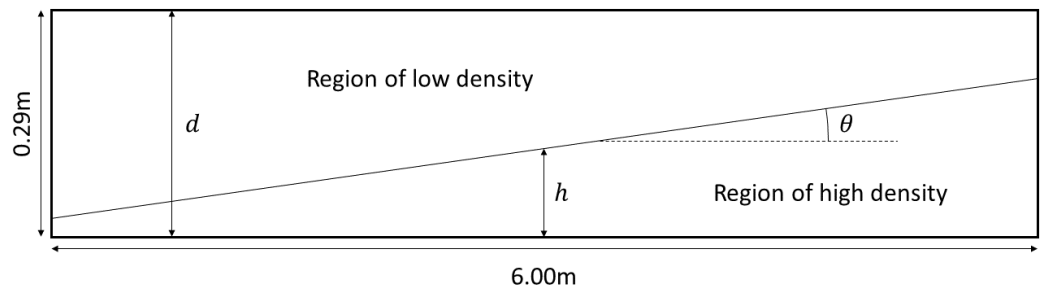


Figure 2.5    A cross-sectional view of the initial condition of the experiments described in Horn et al. (1990). This is not drawn to scale.

The tank is 6.00m long, 0.30m wide and 0.29m deep (see Figure 2.5). Initially the water is stagnant (u=v=w=0). The density difference between the two layers is 20kg/m³ and the interface thickness is 0.01m. Horn et al performed a number of experiments with different values of the depth ratio $h/d$ and of the angle of tilt, $\theta$. Here, the experiments with $h/d = 0.3$ and $\theta = 0.5°, 1.0°$ and $1.5°$ are considered.

## 2.3.2    Set-up

The horizontal mesh consists of uniform quadrilateral elements with one element across the tank and 600 elements along the tank. In the vertical 80 equidistant sigma layers are applied. The thickness of the interface is modelled by linear interpolation of the salinity between the two layers. The duration time for the simulation is 400s. The average time step is 0.002s for both the flow calculation and the advection-diffusion calculation.

Both horizontal and vertical eddy viscosity is applied using a k-epsilon formulation. A bed resistance with a quadratic drag coefficient with a constant value of 0.0175 is applied. For the salinity the scaled eddy viscosity formulation is used for the horizontal and vertical dispersion. The scaling factor is 1 and 0.1, respectively. The simulation is run with a free surface which is different to the experiment which is done with a lid on the tank. Furthermore, there was no wall friction applied during the simulation.

Simulations are performed using both the non-hydrostatic and hydrostatic version of MIKE 3 Flow Model FM. For the hydrostatic version higher-order scheme in time and space is applied.

## 2.3.3    Results

Figure 2.6 shows a time-series of the displacement of the interface between the heavier and lighter fluid near the centre of the tank (x=3.02m). The results presented here show that the simulation captures the main trends seen in the experimental results from Horn et al. (2001), but the velocity and dampening of the waves is underpredicted. One reason for this might be the missing application of wall-friction. Other simulations of the experiment have been reported in e.g. Kanarska et al. (2007), Klingbeil et al. (2013), Stashchuk et al. (2005), Vitousek et al. (2014), and Wadzuk et al. (2004). The results of the present model compare well with the results shown in these papers.
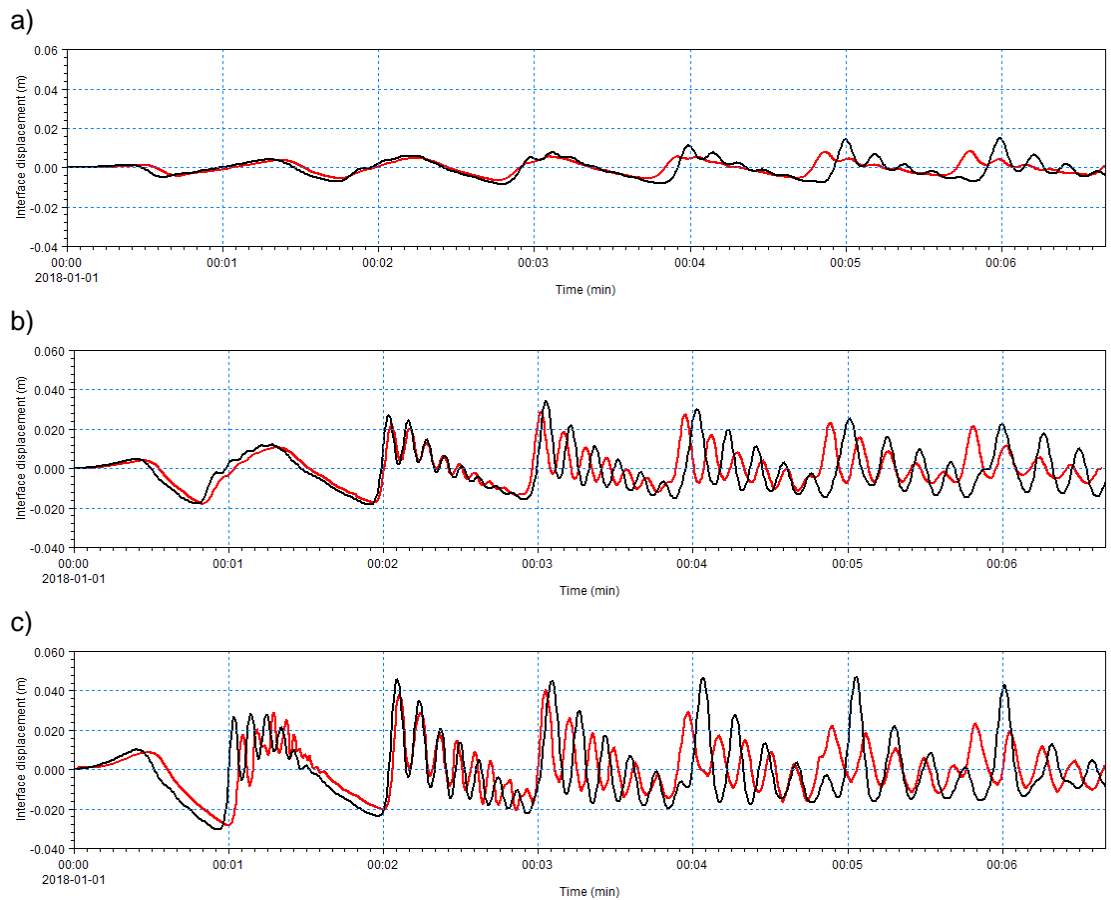
a)



b)



c)



Figure 2.6    Interface displacement at the centre of the tank (x=3.02m). Black line: Non-
             hydrostatic simulation; Red line: experimental data (Horn et al 2001). a)  θ=0.5°. b)
             θ=1.0°. c) θ=1.5°.

Figure 2.7 shows the simulation with the initial interface tilted 1.5° run with both the
hydrostatic and non-hydrostatic version of the MIKE 3 Flow Model FM. This shows that
using the hydrostatic version it is not possible to model the solitons seen both in the
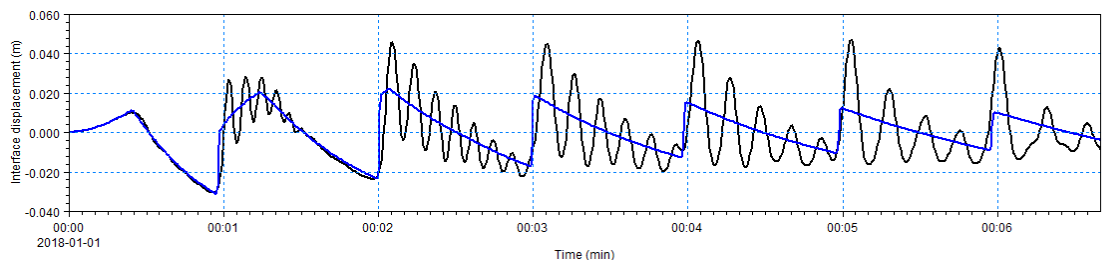experimental data and when modelling with the non-hydrostatic version.



Figure 2.7    Interface displacement at the centre of the tank (x=3.02m) for the case with θ=1.5°.
             Black line: Non-hydrostatic formulation; Blue line: Hydrostatic formulation.

## 2.4 Submerged Hydraulic Jump

### 2.4.1 Description

This test case is a simulation of some of the experimental results described in Long et al. (1990). The experiment consists of a tank at the start of a channel, see Figure 2.8. Between the tank and the channel there is a gate only open at the bottom. This opening allows the water from the tank to flow into the channel and form a submerged hydraulic jump. The bottom of the gate is curved to allow for a more uniform flow into the channel. The water level in the tank is kept constant by pumping water into it. This keeps the discharge into the channel constant. At the end of the channel there is a plate to control the water level. During the experiment the mean water level was measured at different positions in the channel which is what the simulations will be compare to.

The channel is 0.467m wide and 7.5m long. The height of the opening between the bed and the gate, $Y_1$, along with the velocity of the flow into the channel, $U_1$, and the downstream depth, $Y_t$, are all controllable. The result of 10 series of experiments (S1 through S10) each with different conditions on $Y_1$, $U_1$, and $Y_t$ are reported in Long et al. (1990). This test will focus on the following 3 experimental conditions. S3 with $Y_1$=0.025m, $U_1$=1.58m/s, and $Y_t$=0.187m, S6 with $Y_1$=0.025m, $U_1$=2.72m/s, and $Y_t$=0.299m, and S8 with $Y_1$=0.015m, $U_1$=3.14m/s, and $Y_t$=0.206m.
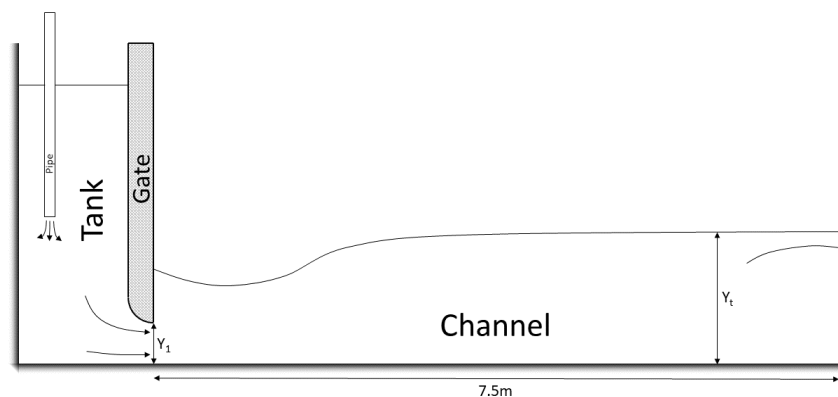


Figure 2.8    A simplified cross-sectional view of the experimental setup from Long et al. (1990). This is not drawn to scale.

The initial conditions of each simulation are stagnant water with a depth equal to $Y_t$. The simulations are run until a steady state is achieved at which point the water level is extracted.

### 2.4.2 Set-up

The simulation differs from the experiment in the following ways. The length of the numerical flume is 6m where the tank is 1m and the channel is 5m. The end of the channel is simulated with an open boundary condition with constant water level. The gate is simulated as a 2D gate with no width and therefore no curved bottom. The discharge pump is modelled using a simple source in the tank.

The horizontal mesh consists of 6300 uniform quadrilateral elements. There are 300 elements over the length of the flume and 21 elements over the width of the flume. In the vertical 20 equidistant sigma layers are applied below which are 12 equidistant z-layers

each with a height of 0.025m for case S3 and S6 and 0.015m for case S8. A mesh with 6301 horizontal elements is also used. Here quadrilateral elements are used in the tank and triangular elements are used in the channel. The same vertical discretization is used as for the first mesh. The duration time for the simulation is 300s and the average time step is 0.003s, 0.002s and 0.002s, respectively, for case S3, S6 and S8. The simple source is located at $(x,y)=(-0.905, 0.2335)$ and layer number 20. The discharge is $0.01475721m^3/s$, $0.02540481m^3/s$ and $0.01759656m^3/s$, respectively, for case S3, S6 and S8. The discharge is reduced with 20% compared to the discharge used in the experiments so that the current speed below the gate corresponds to the velocity in the experiments.

Both horizontal and vertical eddy viscosity is applied using a k-epsilon formulation. A constant roughness height of 0.5mm is applied for the bed resistance. No Coriolis force is applied.
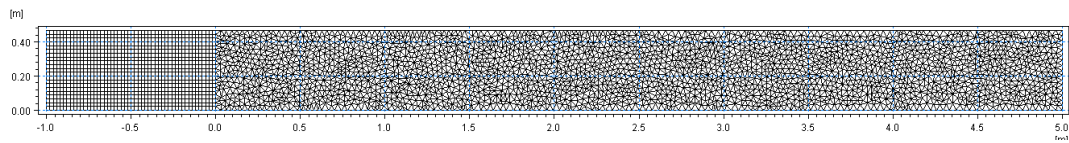


Figure 2.9     Mesh containing a combination of quadrilateral elements and triangular elements.

## 2.4.3    Results

Figure 2.10  shows the velocity field in a cross section along the centreline for the case S8. Figure 2.11 shows the steady state water level at the centreline as function of the distance from the gate. The model results are compared with the experimental results.
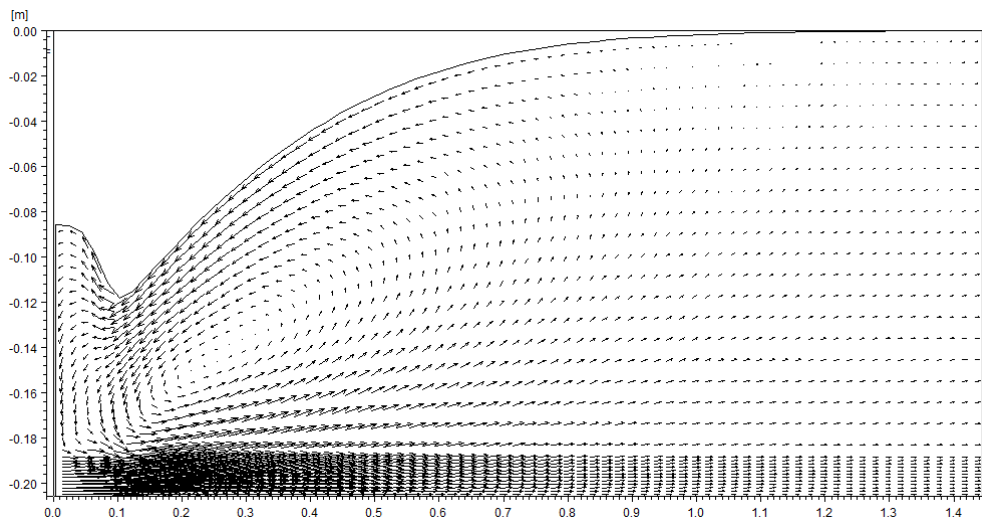


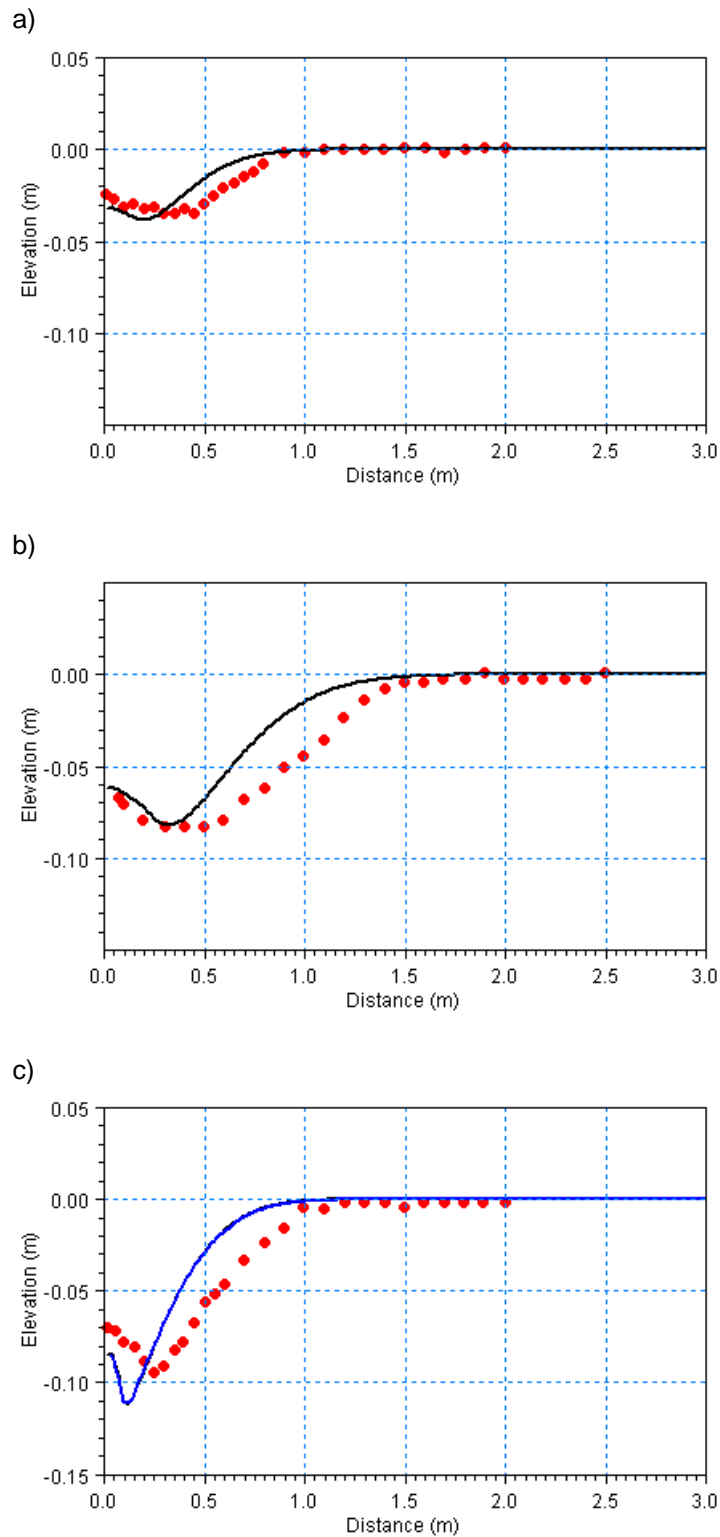Figure 2.10    Velocity field in a cross section along the centreline for the case S8.

a)



b)



c)



Figure 2.11    Mean water level at the centreline as function of the distance from the gate.  a) S3 with $Y_1$=0.025m, $U_1$=1.58m/s. and $Y_f$=0.187m. b) S6 with $Y_1$=0.025m, $U_1$=2.72m/s, and $Y_f$=0.299m. c) S8 with $Y_1$=0.015m, $U_1$=3.14m/s, and $Y_f$=0.206m. Black line: Numerical calculations with the mesh with quadrilateral elements; Blue line: Numerical calculation with a combination of quadrilateral and triangular elements; Red dots: measurements from Long et al (1990).

## 2.5 Dam-break Flow through Sharp Bend

### 2.5.1 Description

A comprehensive experimental study of a dam-break flow in a channel with a 90 degree bend has been reported by Soares-Frazão and Zech (2002, 1999a, 1999b). The setup is shown in Figure 2.12. The width of the two reaches is 0.495m and the length is 3.92m and 2.92m. The channel slope is equal to zero. A guillotine-type gate connects this L-shaped channel to a 2.44m x 2.39m (nearly) square reservoir. The reservoir bottom level is 0.33m lower that the channel bed level. At the downstream boundary a chute is placed. See Figure 2.12 for details.

Soares-Frazão and Zech performed measurements for both dry bed and wet bed conditions. Here comparisons are made for the case where the water in the reservoir is initially at rest, with the free surface 0.20m above the channel bed level, i.e. the water depth in the reservoir is 0.53m. The channel bed is initially dry. The Manning coefficients evaluated through steady-state flow experimentation are $0.0095 s/m^{1/3}$ and $0.0195 s/m^{1/3}$, respectively, for the bed and the walls of the channel.
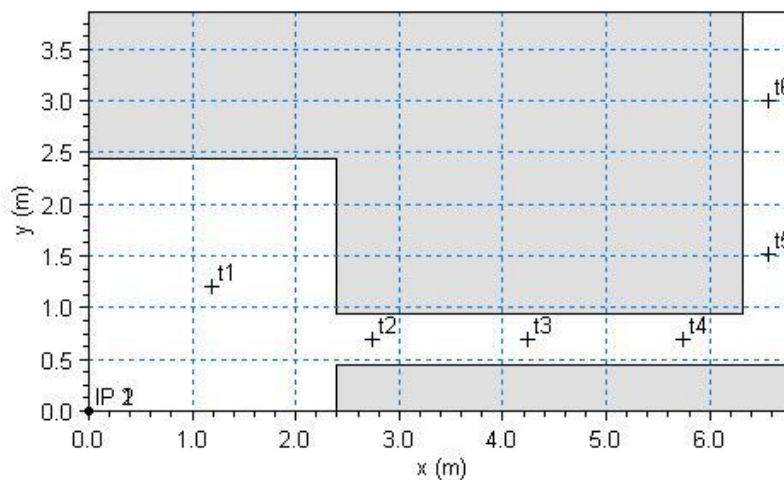


Figure 2.12    Setup of the experiment by Soares-Frazão and Zech (2002)

### 2.5.2 Set-up

An unstructured horizontal mesh is used containing 18311 triangular elements and 9537 nodes. The minimum edge length is 0.01906 m and the maximum edge length is 0.06125 m. In the vertical a sigma/z-level discretization is applied with 9 z-level layers with a constant grid spacing of 0.03m and 10 sigma layers. The duration time is 40s and the average time step is 0.001s.

The wetting depth, and drying depth are 0.002m and 0.0001m, respectively. Both horizontal and vertical eddy viscosity are applied using a k-epsilon formulation. A constant roughness height of 0.5mm is applied for the bed resistance. At the downstream boundary, a free outfall boundary condition is applied.

Table 2.1    Location of the gauging points

| Location | x (m) | y (m) |
|----------|-------|-------|
| T1 | 1.19 | 1.20 |
| T2 | 2.74 | 0.69 |
| T3 | 4.24 | 0.69 |
| T4 | 5.74 | 0.69 |
| T5 | 6.56 | 1.51 |
| T6 | 6.56 | 3.01 |

## 2.5.3    Results

In Figure 2.13 time series of calculated surface elevations at the six gauges locations are compared to the measurements. The agreement with measurements is very good.
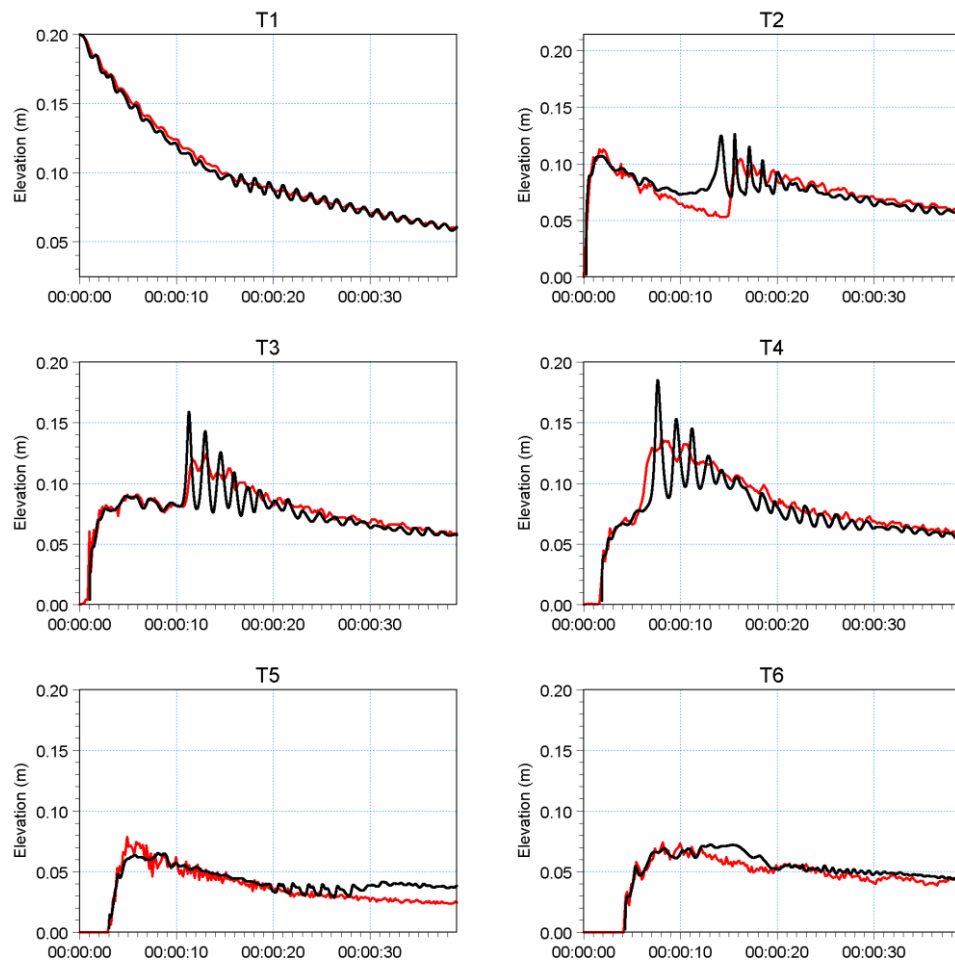


Figure 2.13    Time evolution of the water level at the six gauge locations. Black line: Mon-hydrostatic simulation; Blue line: Hydrostatic simulation; Red line: Measurements by Soares-Frazão and Zech (1999a,b).

## 2.6 Density driven plumes

### 2.6.1 Description

Simulating the nearfield behaviour of sediment disposal plume, specifically its impact on the seabed, the resulting shear stress over the seabed and consequently the deposition/erosion foot-print of sediments has always been a modelling challenge.

This test case is a simulation of the laboratory experiment of dredged material disposal conducted by Jiang and Kunisu (1997). The flume is 4m long and 2m wide. Experiments was performed with a range of different water depths. Here the experiment with the water depth of 0.5m is considered. The experimental setup is shown in Figure 2.14. The disposal volume is 2000cm$^3$. The specific gravity of the disposal sediment is 2.75 and the water content is 145%. In Figure 2.15 a snapshot of the experiment is showing the plume impact and the resulting density current over the bottom.
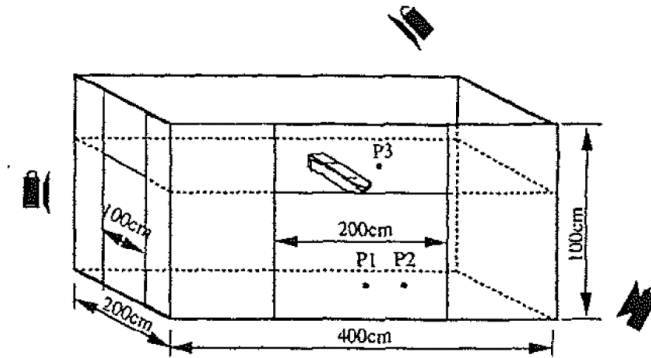


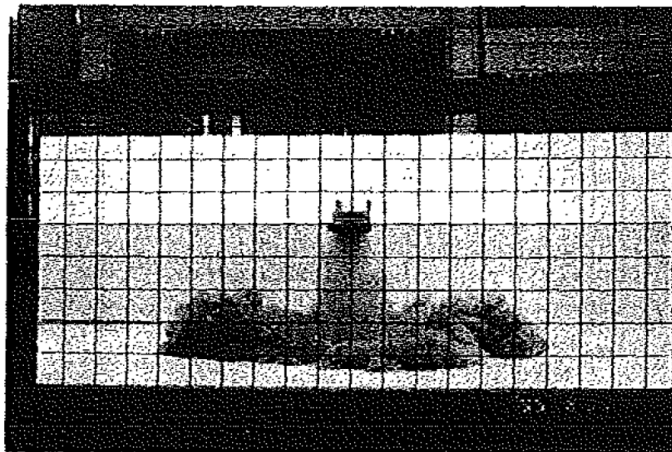Figure 2.14    Sketch of experimental setup (Jiang and Kunisu, 1997).



Figure 2.15    Snapshot from the experiment (Jiang and Kunisu, 1997)

### 2.6.2 Setup

The horizontal mesh consists of 5000 quadrilateral elements with 50 elements across the flume and 100 along flume. In the vertical 50 equidistant sigma layers are applied. The duration time for the simulation is 60s with an average time step of 0.0043s for the flow calculations.

Both horizontal and vertical eddy viscosity are applied using a k-epsilon formulation. A constant roughness height of 1mm is applied for the bed resistance. No Coriolis force is applied. For the salinity the scaled eddy viscosity formulation is used for the horizontal and vertical dispersion. The scaling factor is 1.0 for the horizontal dispersion and 0.1 for vertical dispersion.

The Mud Transport module is activated with density feedback to the Hydrodynamic module. The initial density of water is set to 1024.61 (temperature T=10°C and salinity S=32PSU). In order to simulate the instant release of disposal material into the water, the initial condition for the suspended sediment concentration is defined as shown in Figure 2.16. The concentration of the disposed material is 550kg/m$^3$ and a background concentration of 0kg/m$^3$ is applied.
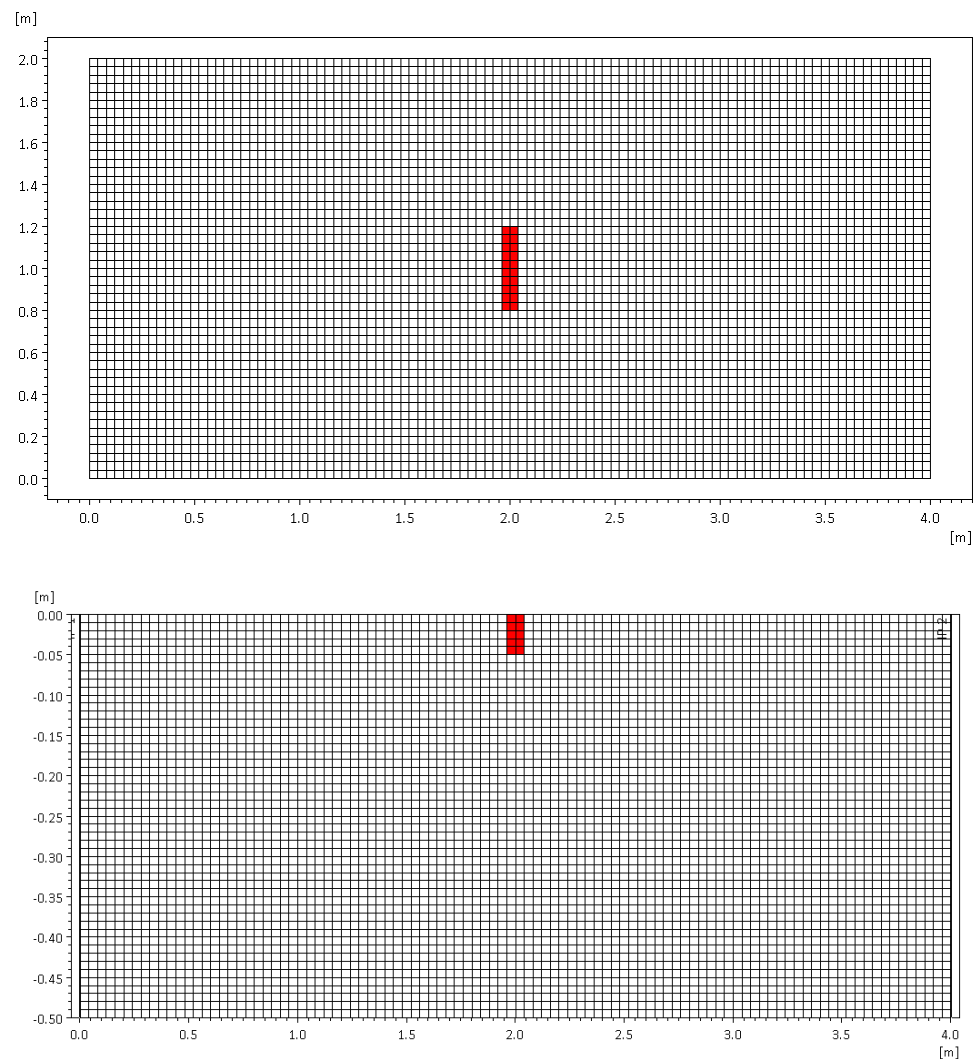


Figure 2.16    Model initial conditions. Plan view (top) and vertical cross-section (bottom).

## 2.6.3    Results

In Figure 2.17 the measured current speeds at point P1(x=2.2m, y=1.0m, z=-0.45m) are compared with the model results. The peak velocity occurs when the density surge passes

by this point. The model underpredicts the peak of the velocities close to the seabed compared to the measurements.
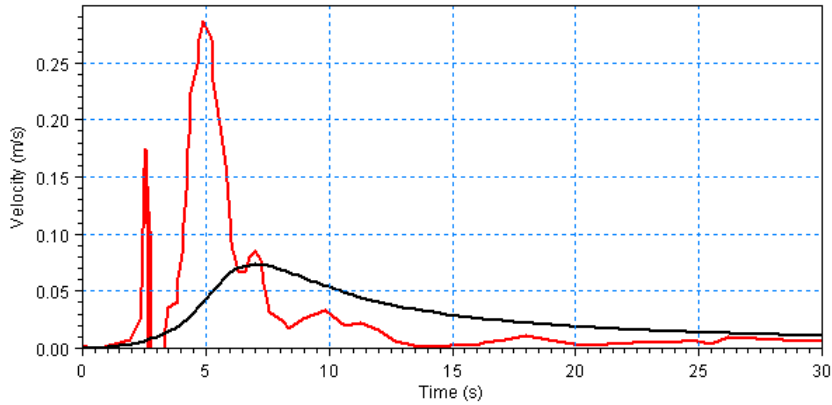


Figure 2.17    Current speeds at P1. Comparison between measured and model. Blue line: Non-hydrostatic calculations. Red line: Experimental data by Jiang and Kunisu, 1997.

In Figure 2.18 and Figure 2.19 snapshots of model results at t=10s and 20s are shown in the vertical profile from (0.5,1) to (3.5,1). The plots show the suspended sediment concentrations (SSC) and the velocity field.
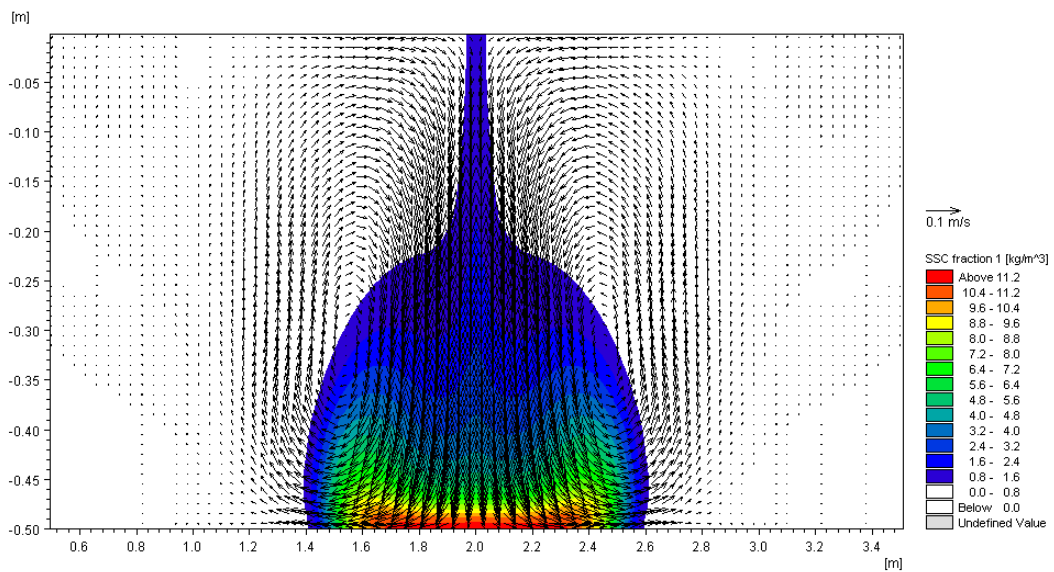


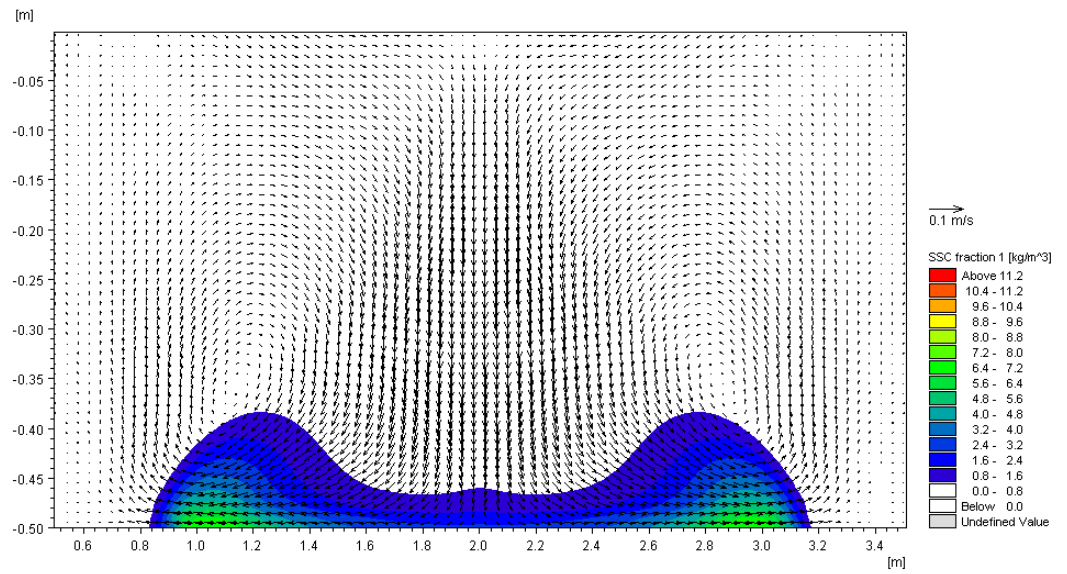Figure 2.18    Vertical profile at t=10s of the suspended sediment concentration (SSC) and the velocity field.

Figure 2.19    Vertical profile at t=20s of the suspended sediment concentration (SSC) and the velocity field.

# 3    References

/1/    Fringer, O. B., M. Gerritsen and R.L. Street (2006), An unstructured-grid, finite volume, nonhydrostatic, parallel coastal ocean simulator, Ocean Modelling ,**14**, 139-173.

/2/    Horn D.A., Imberger J., Ivey G.N. (2001), The degeneration of large-scale interfacial gravity waves in lakes, J. Fluid Mech., 434, 181–207.

/3/    Härtel, C., Meiburg E., Necker F. (2000), Analysis and direct numerical simulation of the flow at a gravity-current head: Part 1 Flow topology and front speed for slip and no-slip boundaries, J. Fluid Mech., 418, 189-212.

/4/    Jiang, Q., Kunisu, H. and Watanabe, A. (1997), Numerical modelling of the settling processes of dredged material disposed in open waters. In *The Seventh International Offshore and Polar Engineering Conference*. International Society of Offshore and Polar Engineers.

/5/    Kanarska Y., Shchepetkin A., McWilliams J.C. (2007), Algorithm for non-hydrostatic dynamics in the Regional Oceanic Modeling System, Ocean Modelling, 18, 143–174.

/6/    Klingbeil K., Burchard H. (2013), Implementation of a direct nonhydrostatic pressure gradient discretisation into a layered ocean model, Ocean Modelling, 65, 65–77.

/7/    Lai, Z., Chen C., Cowles G.W., Beardsley R.C. (2010), A nonhydrostatic version of FVCOM: 1. Validation experiments, J. Geophys. Res., 115.

/8/    Long D., Steffler P.M., Rajaratnam N.  (1990), LDA study of flow structure in submerged hydraulic jump, Journal of Hydraulic Research, 28:4, 437-460, DOI: 10.1080/00221689009499059.

/9/    Soares-Frazão, S. and Zech, Y. (2002), Dam-break in channel with 90° bend, Journal of Hydraulic Engineering, ASCE, 2002, 128, No. 11, 956-968.

/10/   Soares-Frazão, S. and Zech, Y. (1999a), Effects of a sharp bend on dam-break flow, Proc., 28th IAHR Congress, Graz, Austria, Technical Univ. Graz, Graz, Austria (CD-Rom).

/11/   Soares-Frazão, S. and Zech, Y. (1999b), Dam-break flow through sharp bends – Physical model and 2D Boltzmann model validation, Proc., CADAM Meeting Wallingford, U.K., 2-3 March 1998, European Commission, Brussels, Belgium, 151-169.

/12/   Stashchuk N., Vlasenko V., Hutter K., (2005), Numerical modelling of disintegration of basin-scale internal waves in a tank filled with stratified water. Nonlinear Processes in Geophysics, European Geosciences Union (EGU), 12 (6), pp.955-964. <hal-00302667>.

/13/   UNESCO (1981), The practical salinity scale 1978 and the international equation of state of seawater 1980, UNESCO technical papers in marine science, 36, 1981.

/14/   Vitousek S., Fringer O.B. (2014), A nonhydrostatic, isopycnal-coordinate ocean model for internal waves, Ocean Modelling 83, 118–144.

/15/     Wadzuk, B.M, Hodges B.R. (2004), Hydrostatic and Non-hydrostatic Internal Wave Models, CRWR Online Report 04-09, Center for Research in Water Resources, University of Texas at Austin, 77 pages, http://www.crwr.utexas.edu/online.html.